Test of PV inverters under unbalanced operation

Wang, Ziyu; Rasmussen, Theis Bo; Yang, Guangya

Published in:
The Journal of Engineering

Link to article, DOI:
10.1049/joe.2018.9308

Publication date:
2019

Document Version
Publisher's PDF, also known as Version of record

The Journal of Engineering

The 7th International Conference on Renewable Power Generation (RPG 2018)

Test of PV inverters under unbalanced operation

eISSN 2051-3305
Received on 29th October 2018
Accepted on 9th January 2019
E-First on 4th June 2019
doi: 10.1049/joe.2018.9308
www.ietdl.org

Ziyu Wang[1] ✉, Theis Bo Rasmussen[1], Guangya Yang[1]
[1]*Technical University of Denmark (DTU), Centre for Electric power and Energy (CEE), Denmark*
✉ *E-mail: ziywa@elektro.dtu.dk*

Abstract: In the modern renewable energy system, recent years have seen a rise in the share of power being generated through photovoltaic (PV) plants. In the Danish power system, PV plants are mostly integrated in the medium- and low-voltage networks which are usually operating under unbalanced conditions. Furthermore, the increasing number of power-electronic-based equipment affects the grid during faults through their contribution to the fault current. So far studies of PV plants in unbalanced conditions are based on computational simulations, which have limitations in representing reality. Therefore, this study investigated the performance of a three-phase PV inverter under unbalanced operation and fault conditions. The inverter is tested in stable power system operation and during grid support situations through frequency response and reactive power control. All experiments are carried out using an experimental laboratory platform in PowerLabDK. The key outcomes from this study includes the correlation between positive sequence component of voltage and reactive power, active power and current under unbalanced operation, the frequency response dependence on positive sequence voltage, and the fault current contribution from PV inverter during different fault conditions.

1 Introduction

With the development of renewable energy technology during the last decades, more and more distributed energy resources (DERs) are integrated into the power systems, especially wind and solar energy. Thanks to the abundant resources and zero carbon emission, solar photovoltaic (PV) energy has now become a significant renewable energy technology. In Denmark, the installation capacity of solar PV has reached 924 MW by April 2018 equivalent to about 6.5% of the total production capacity.

Currently in Denmark, there are mainly two grid codes for PV plants of different capacities, i.e. Technical Regulation 3.2.1 (TR 3.2.1) for power plants up to and including 11 kW and Technical Regulation 3.2.2 (TR 3.2.2) for PV power plants above 11 kW published by the Danish transmission system operator (TSO) Energinet. In the perspective of international standard, in International Electrotechnical Commission (IEC), the PV system grid-connection and testing follow wind turbine standards, such as IEC61400-21.

In the recent decade, multiple studies in PV plants have been conducted in different perspectives. Part of these studies are done from an inverter perspective, including maximum power point tracking (MPPT) algorithm and control strategies, while others concentrate on the power system perspective, i.e. integration technologies, such as power quality and voltage regulation, and fault conditions. The studies conducted in [1, 2] have investigated the validity of PV simulation models based on hardware experiments, where the experiment in [2] have utilised a simplified PV inverter circuit to build a 13-stage inverter. The studies in [3–9] conducted studies on the effects and contributions introduced by PV system integration into the power system. The work done in [3–6] have studied the voltage-rise problem caused by PV systems and the mitigation methods, including reactive power support and peak shaving with energy storage facilities. The researches in [7, 8] present different types of PV inverters and their requirements for integration. The work in [9] studied the integration of PV-system-based hardware but concentrates on balanced operation and only fault ride-through (FRT) capability in terms of fault conditions. Studies in [10, 11] have conducted investigations on non-uniform conditions including unbalanced voltage sags and faults. These studies are conducted based on simulation, meaning that the models are built for intended use and are to a certain degree simplified.

As of limitations of the laboratory environment and economic issues, most studies are conducted based on simulation software or small-scale simplified hardware setups and are not considering real hardware platforms. Furthermore, when it comes to the studies of the non-uniform or transient conditions of the inverter, existing commercial simulation tools are not able to model a complete inverter and the complex behaviours under such conditions rigorously and precisely because of various technical burdens [10].

In the Danish power system, PV power plants are mainly installed in residential areas, as small-scale roof-top PV modules, which means that they are integrated into the distribution grid at low voltage (LV). Since LV networks usually operate under unbalanced conditions, it is meaningful to investigate the performance of three-phase PV inverters under unbalanced conditions, including its dynamic reactive power control, dynamic power factor control, and primary frequency regulation. Furthermore, it is essential to evaluate the fault current contribution from the PV systems during different fault conditions.

With the laboratory facilities provided by PowerLabDK, it is possible to perform the tests on a real hardware platform. Here, a series of experiments are conducted with the objective to investigate the PV inverter performances under unbalanced operation and fault conditions. The effect of positive sequence voltage on the performance has been found. In Section 2, the method including experiment platform and test setup are to be introduced. The test results and analysis are presented in Section 3, and Section 4 concludes from the results.

2 Methodology

The simulation models of complex equipment, such as PV inverters, are only as accurate as the intended purpose suggests. Real structure and topology of PV inverters can be far more complicated. Furthermore, PV inverters are designed to follow the current grid codes, which in Denmark have limited requirements during unbalanced operation and faults.

This study and configuration of experiments follow the Technical Regulation 3.2.1 (TR 3.2.1) of the Danish Grid codes published by the national TSO, Energinet [11]. According to TR 3.2.1, the requirements during unbalanced conditions indicate that

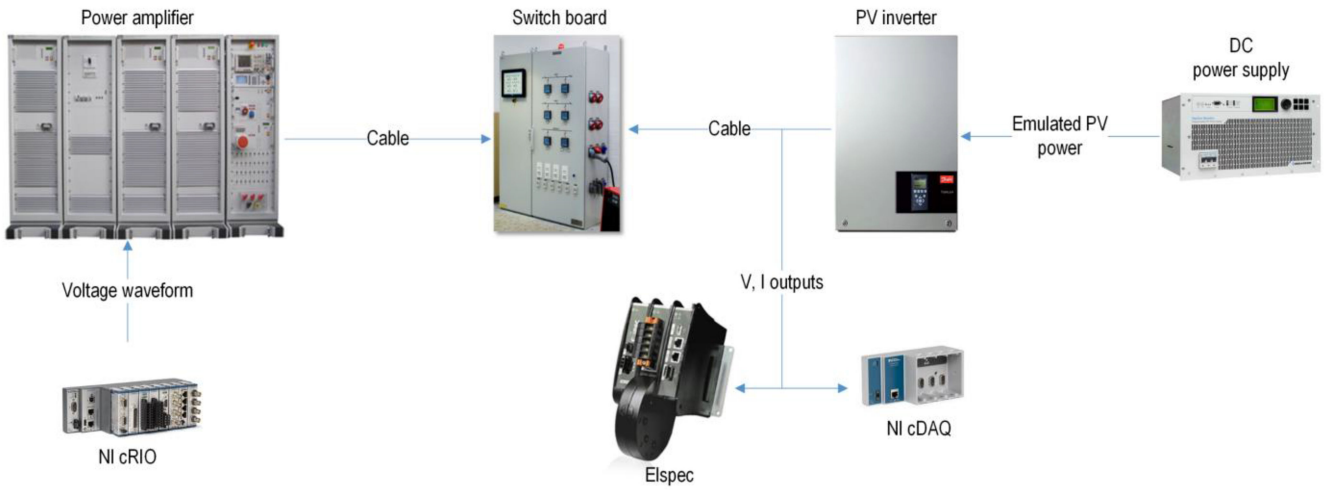

Fig. 1 *PowerLabDK PV inverter experimental platform overview*

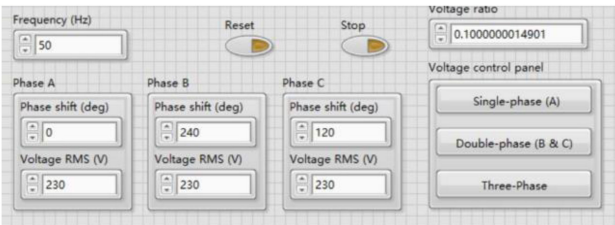

Fig. 2 *cRIO control panel as human-machine interface*

'the asymmetry between phases under both normal operation and fault conditions should not exceed 16 A'. Furthermore, as part of the modern power system, PV plants integrated in Denmark are required to support the operation of the power grid during frequency deviation. This requirement is described in TR 3.2.1 by the activation of droop-based primary frequency response when the system frequency is between 50 and 52 Hz and must respond within 2s with a droop rate of between 2% and 12% of the nominal active power of the PV plant [11].

2.1 Laboratory testing platform

The compliance of the specific PV inverter in the laboratory at PowerLabDK, with the Danish grid codes can be investigated through the design of several test situations and the establishment of an experimental test platform. An overview of the laboratory setup is shown in Fig. 1.

To realise the designed test situations, specific voltage profiles at the terminal of the inverter, including different unbalanced and fault conditions must be generated. The 150 kVA power amplifiers in Fig. 1 allow this by forming a three-phase controllable grid connected to the PV inverter through lab cells represented by the switch board in Fig. 1. The input voltage, both magnitude and phase angle, of each phase is controlled by National Instruments (NI) CompactRIO (cRIO) in Fig. 1. An ELSPEC meter is installed at the terminals of the inverter to measure the output from the inverter and save the measurements on the dedicated server. During the fault condition test, the output voltage and current are also measured by NI CompactDAQ (cDAQ) for raw data acquisition. Since the output from real PV modules is intermittent and directly depending on the irradiance level and ambient temperature, a programmable DC power supply shown in Fig. 1 is used instead of the PV modules, to get a more stable input into the inverter and increase the controllability of the testing platform.

The NI cRIO is programmed in NI LabVIEW and made capable of controlling the magnitude and phase angle of three analogue output channels of the NI-9269 voltage module, through the human–machine interface (HMI) shown in Fig. 2. Here, 'voltage ratio' is defined as the per unit value of the desired voltage, namely the ratio between desired voltage and inverter nominal voltage. The value is entered in the text box at the right side of Fig. 2 and by clicking on of the buttons in the middle, the fault or unbalanced conditions are applied to the corresponding phase(s). The frequency is controlled by entering values in the text box in the top left corner of Fig. 2. Since the power generation from PV power plants is usually high when the demand is low and due to the over-frequency support requirements in TR 3.2.1 only over-frequency conditions are tested in the experiments.

2.2 Experiment configurations

With the laboratory setup in Fig. 1, several experiments are conducted in both balanced and unbalanced operation and during fault conditions. For the test conducted with balanced conditions, all three phases have equal voltage magnitude. For the balanced operation conditions, it is further assumed that the base voltage is defined as 230 V line to neutral and the active power output of the PV inverter is controlled to be 10 kW through the programmable DC power supply. In balanced operation conditions, a total of 16 tests are conducted with the voltage magnitude changing from 0.93 per unit (pu) to 1.09 pu, with increments of 0.01 pu. The balanced operation tests serve as a benchmark for the subsequent unbalanced operating condition experiments performed as follows:

i. Single-phase (Phase A) unbalance

   a. Dynamic reactive power support ($Q(V)$ control)
   b. Dynamic power factor support ($PF(P)$ control)
   c. Primary frequency support

ii. Double-phase (Phase B and C) unbalance

   a. Dynamic reactive power support ($Q(V)$ control)
   b. Dynamic power factor support ($PF(P)$ control)
   c. Primary frequency support

As in the benchmark conditions, the unbalanced operation tests are performed with the voltage of the unbalanced phase(s) equal to 0.93 pu to 1.09 pu, with increments of 0.01 pu and each value stays for 30s. Furthermore, the voltage base and active power output of the inverter are defined equal to those used in the balanced test cases. In the unbalanced operation tests, the voltage magnitude of the remaining phase(s) is kept constant at 1 pu. For all test conducted in this study, it is only the voltage magnitude that is unbalanced and the voltage angle between the phases is kept constant at 120°. In the primary frequency response test for both balanced and unbalanced conditions, the voltage of the unbalanced phases is controlled at 0.95 pu and 1.05 pu, while the remaining phase(s) are maintained at unity voltage magnitude.

As mentioned in Section 1, it is important to evaluate the performance of the PV inverter in fault conditions as well, to verify its compliance with the Danish grid codes and to

investigate its contribution through fault currents. Therefore, the inverter is tested in the following fault conditions:

a. Balanced fault
b. Single-phase (Phase A) fault
c. Double-phase (Phase B and C) fault

The fault conditions are simulated by instantly decreasing the voltage to 0.1 pu for the specific phase(s). The short-circuit current contribution from the inverter is investigated for five different active power output ($P_{O:\mathrm{inv}}$) levels, namely 1.5 kW, 3 kW, 5 kW, 7, and 10 kW. This is emulated by implementing the PV characteristics shown in Fig. 3 on the DC power supply. Fig. 3 clearly shows five *I-V* curves have identical open-circuit voltage (V_{OC}) but different short-circuit current (). In this way, the PV module output power is emulated with constant ambient temperature but different irradiance levels.

3 Results

Based on the experiments described in Section 2.2, the performance of the three-phase PV inverter in PowerLabDK can be analysed by considering the phase and sequence components of the voltage and current and the active and reactive power output from the inverter.

From the 16 tests conducted with all three phases in balance at different voltage magnitudes, the inverter performed as expected as its current output was controlled to maintain constant active power during the changes in voltage magnitude. Furthermore, the reactive power control system ensured the expected grid support through injection of reactive power during LV magnitude and absorption of reactive power when the terminal voltage exceeded 1 pu. These benchmark results are used throughout the following section as a comparison to the unbalanced operation cases. After the analysis of the inverter performance during unbalanced operation, its response to balanced and unbalanced faults is investigated in Section 3.2.

3.1 Unbalanced operation

Comparing the single- and double-phase unbalanced conditions, and the balanced operation tests conducted with the PV inverter operating in $Q(V)$ reactive power control mode, reveals a relationship between the positive sequence, denoted by subscript *1*, voltage and current, as shown in Figs. 4*a* and *b*.

The *x*-axis in Figs. 4*a* and *b* describes the voltage ratio between the voltage of the phase(s) which are changing in the specific scenario V_{Δ} and the nominal voltage. In the balanced test, represented by the subscript *b*, the voltage of all phases changes simultaneously, while in the single-phase unbalance, denoted by subscript *s*, only phase A voltage changes, and in the double-phase unbalance, denoted by subscript *d*, only phases B and C voltage changes.

Furthermore, from the positive sequence results shown in Figs. 4*a* and *b*, it can be observed that even though the input voltage waveforms from the cRIO to the three-phase amplifier was set with increments of 0.01 pu at a per unit voltage base of 230, the voltage at the terminals of the inverter is around 0.004 pu higher, that is at 0.93 pu input voltage, the measured voltage was 0.934 pu. This is partly due to small oscillations in the amplifier output of around pu, seen on the equipment from panel, and due to the voltage rise caused by the PV inverter operating at its rated output of 10 kW.

The results in Fig. 4*a* clearly show that regardless of the balancing conditions between the phases, the positive sequence voltage has a linear relationship with the voltage ratio between V_{Δ} and V_N. Furthermore, the positive sequence currents in Fig. 4*b* shows its inverse relationship with the voltage ratio.

A comparison of the reactive power response to the off-nominal voltage ratio in the balanced and unbalanced conditions further shows that the $Q(V)$ control depends on the positive sequence voltage as shown in Fig. 5, where the total reactive power output of the amplifier is shown in the three balancing conditions.

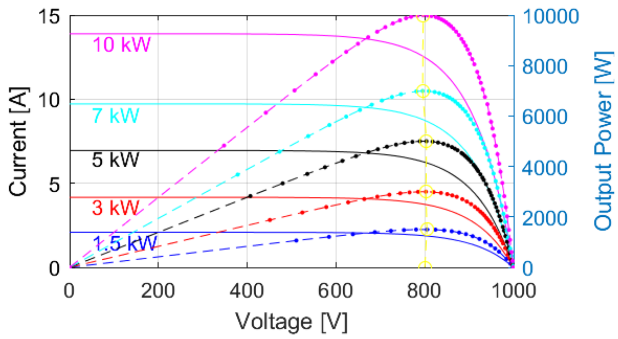

Fig. 3 *PV inverter I-V and P-V curves for different output power levels, representing different irradiance levels*

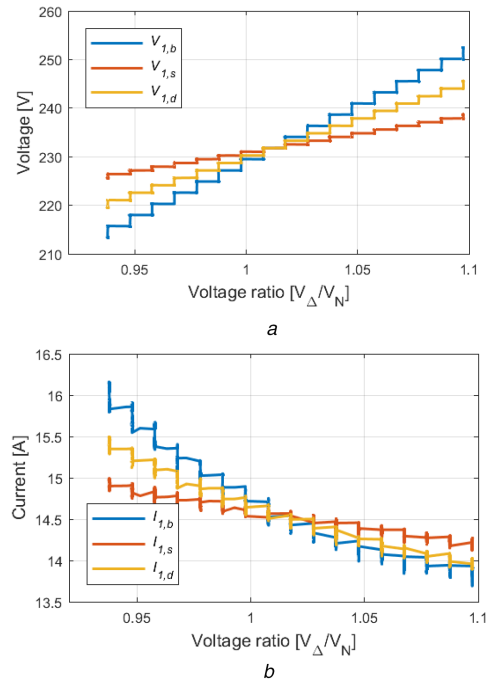

Fig. 4 *Positive sequence voltage and current for balanced, single-phase unbalanced, and double-phase unbalanced operation*
(a) Positive sequence voltage ***(b)*** Positive sequence current

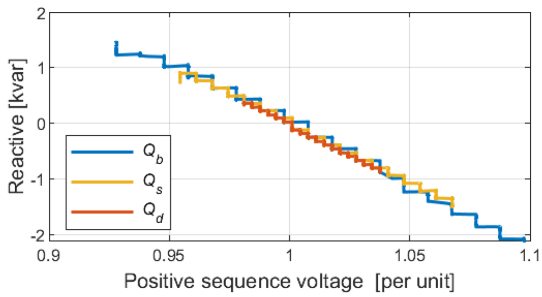

Fig. 5 *Reactive power output of inverter during Q(V) control for balanced, single-phase unbalanced, and double-phase unbalanced operation*

It is observed in Fig. 5, that in the under-voltage area (below nominal), the inverter supports the system by injecting inductive reactive power while it injects capacitive or absorbs reactive power within the over-voltage zone (above nominal). With the *x*-axis of Fig. 5 being the positive sequence voltage from Fig. 4*a*, it can be verified that the amount of total reactive power output from the inverter is directly controlled by the positive sequence component of voltage. The amount of Q under unbalanced operation is proportional to that under balanced operation. The amount of Q_b is three times the Q_s and 1.5 times the Q_d.

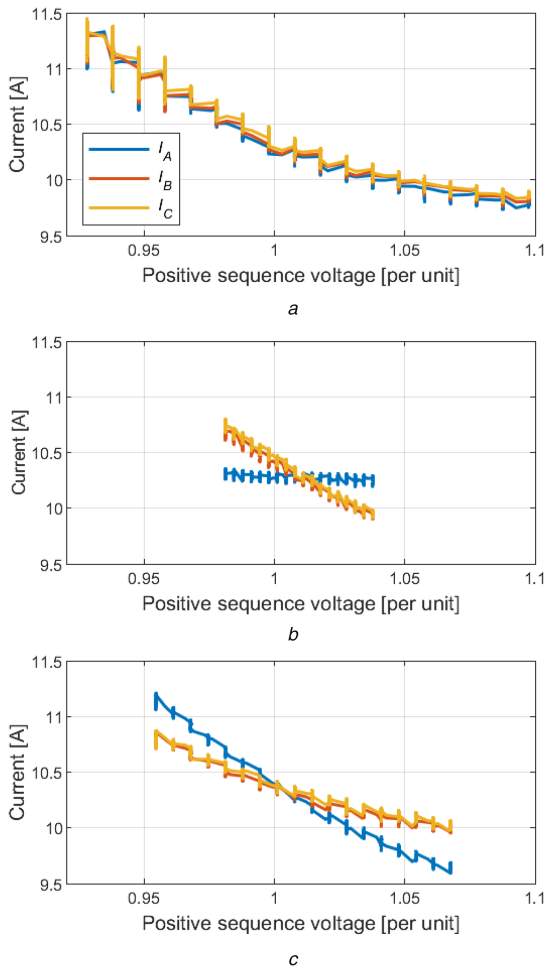

Fig. 6 *Per phase RMS current for balanced, single-phase unbalanced, and double-phase unbalanced operation conditions*
(a) Balanced operation RMS current ***(b)*** Single-phase unbalanced operation RMS current ***(c)*** Double-phase unbalance operation RMS current

The root mean square (RMS) values of the current of each phase are shown in Figs. 6*a*–*c*, for the balanced, single-phase unbalanced, double-phase unbalanced operation, respectively. From Fig. 6*a*, it is clear that the current of three phases decreases in the same trend as the positive sequence component of voltage increases. However, under unbalanced operation, as shown in Figs. 6*b* and *c*, the current of the balanced phase(s) drops more than the unbalanced phase(s) as the positive sequence component of voltage increases. The output current of the inverter is directly controlled by the positive sequence component of the voltage. The largest current difference between phases is 0.5 A, which comply with the requirement in TR 3.2.1.

As of the changes in the current, the active power output of the unbalanced phase(s) increases while that of the balanced phase(s) decreases. Consequently, the total active power output maintains at an approximate constant level as the voltage unbalanced degree changes. The differences between the application of $Q(V)$ and PF*(P)* control are compared in Fig. 7 for the single- and double-phase unbalanced operation conditions.

With PF(P) control applied, the reactive power output is kept constant while it changes in $Q(V)$ control as the positive sequence component of the voltage increases. Since the active power output is constant, the power factor is also constant under PF(P) control. Thus, the reactive power under PF(P) control is constant as shown in Fig. 7.

The results of the over-frequency support test are plotted in Figs. 8*a* and *b*. The *x*-axis in Fig. 8 represents the increment in frequency from 50 to 51 Hz with increment of 0.1 Hz. According to Fig. 8*a*, the active power generation starts responding to the over frequency at 50.4 Hz, 50.4 and 50.5 Hz for balanced, single-phase, and double-phase unbalanced conditions, respectively, while it

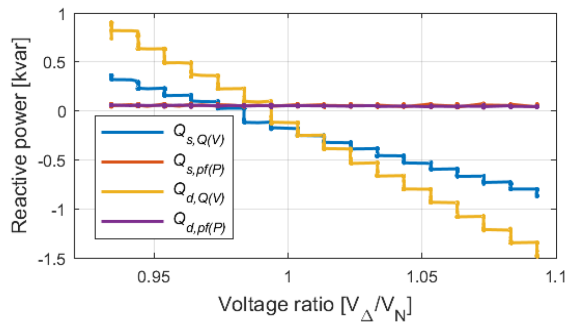

Fig. 7 *Comparison of reactive power output during single- and double-phase unbalanced operation for Q(V) and PF(P) control*

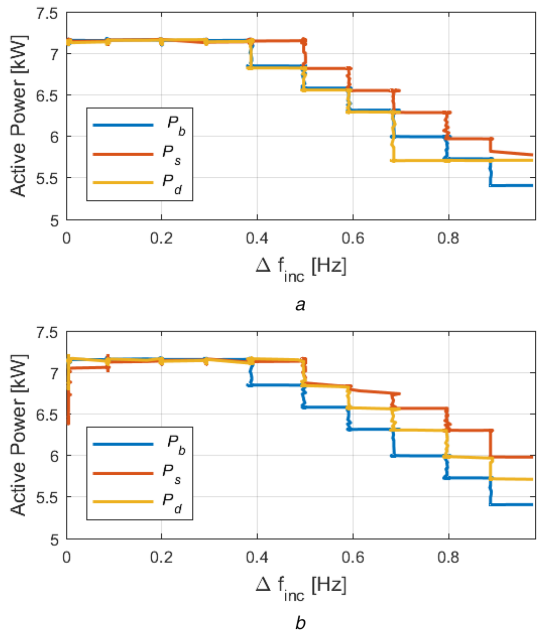

Fig. 8 *Response to positive change in frequency from 50 to 51 Hz, for balanced, single-phase unbalanced and double-phase unbalanced operation*
(a) Voltage magnitude of $V_\Delta = 0.95$ pu ***(b)*** Voltage magnitude of $V_\Delta = 1.05$ pu

responds at 50.4 Hz, 50.5, and 50.5 Hz in Fig. 8*b*. The frequency support function is activated later when the inverter operates under single-phase unbalanced condition during an under-voltage situation and this delay appears in both unbalanced conditions during an over-voltage situation. Although with delay, the activation point is still within the requirement in TR 3.2.1 which is between 50 and 52 Hz.

One of the possible reasons behind the difference in response during balanced and unbalanced operation is the frequency detection technique and the internal control strategies of the inverter. Different from synchronous generators, which detect the frequency deviation based on the difference between mechanical torque and electromagnetic torque, the PV inverters detects frequency deviation by means of phase-locked loop (PLL). The PLL integrated in an inverter can be either a three-phase type or three single-phase ones. The single-phase type uses a positive sequence voltage extractor to acquire the positive sequence voltage of each phase and the frequency is detected at each phase separately. By this means, the inverter responses the frequency deviation based on the per phase positive sequence active power calculated with the positive sequence voltage. During an unbalanced operation, positive sequence voltage and current are lower than that in balanced condition, as indicated in Fig. 4. Therefore, the positive sequence active power is lower and thereof the power reference for frequency regulation is lower which can affect adjusting active power. Therefore, the unbalanced in each phase may affect the performance of the frequency detection function. Another possible reason can be the sudden variation in

Table 1 Fault condition test results

Quantity types	Fault types	Active power output, kW				
		1.5	3	5	7	10
peak fault current [A]	balanced	37.16	44.43	39.27	37.84	39.03
	single phase	31.75	38.13	32.16	38.76	38.25
	double phase	30.23	34.95	36.94	36.74	37.09
disconnection time [s]	balanced	0.66	0.67	0.75	0.64	0.68
	single phase	0.71	0.61	0.79	0.64	0.86
	double-phase	0.70	0.69	0.81	0.71	0.68

the frequency used in the experiment which, in reality, rarely happens.

3.2 Fault conditions

The results of the fault condition tests are included in Table 1. From the first three rows of Table 1, it can be clearly seen that generally the fault current contribution of the balanced fault is the highest while that of the double-phase fault is the lowest. Compared with its nominal peak current 20.5 A calculated with its full capacity and nominal voltage, the fault current can reach about the two times the nominal. The inverter can contribute considerably high fault current to the grid enabling the protection scheme to detect the fault and trip protection mechanism. Additionally, it is observed that the fault current is not affected by the actual active power output. Therefore, it is implied that the fault current contribution is determined by the full capacity of the inverter.

The results in the next three rows have shown the time it takes the inverter to get disconnected during a fault. Generally, the time for the balanced fault condition is the shortest while it is somewhat similar for the unbalanced faults.

4 Conclusion

In this study, a series of experiments are performed on a PV inverter system to investigate its performance under unbalanced operation and different fault conditions. As of the increasing penetration of solar PV inverters at LV network in distribution grid which usually operates in unbalanced condition, the results are beneficial for further study on protection and integration.

During unbalanced operations, with $Q(V)$ control applied, the PV inverter reacts to the under- and over-voltage situations by generating and absorbing reactive power. The amount of the reactive power is controlled by the positive sequence voltage and proportional to that under the balanced operation. The active power output maintains at constant level, indicating that the control strategy of the inverter is to guarantee the active power production. With the PF(P) control applied, the power factor maintains constant due to the constant active power.

By comparing balanced, single-phase unbalanced and double-phase unbalanced conditions, the frequency response function is affected by the unbalanced operation regarding the activation of the support. The function responds slower under the unbalanced conditions. This is likely caused by the change in reference active power caused by the change in positive sequence voltage. Although there are effects on the function, the activation point is still in compliance with Technical Regulation 3.2.1.

During all three fault conditions, the inverter contributes fault current into the grid enabling protection schemes to detect the fault and trip the breakers to clear it. The fault current is the highest in balanced fault while the lowest in double-phase fault, and the fault current is regardless the actual active power output but affected by the full capacity of the inverter. The fault current affects the disconnection time of the inverter. Higher fault current leads to shorter disconnection time.

5 Acknowledgments

The work is supported by Danish ForskEL project ‘A Live PV Testing Platform for Larger Adoption’, grant no. 12421.

6 References

[1] Bravo, R.J., Yinger, R., Robles, S., *et al.*: ‘Solar PV inverter testing for model verification’. Proc. IEEE Power and Energy Society General Meeting, San Diego, CA, July 2011

[2] Loukriz, A., Dudley, S., Brown, R., *et al.*: ‘Experimental validation of a thirteen level H-bridge photovoltaic inverter configuration’. Proc. Int. Conf. Environment and Engineering, Milan, Italy, June 2017

[3] Yang, G., Marra, F., Juamperez, M., *et al.*: ‘Voltage rise mitigation for solar PV integration at LV grids’, *J. Mod. Power Syst. Clean Energy*, 2015, **3**, pp. 411–421

[4] Juamperez, M., Yang, G., Kjaer, S.B.: ‘Voltage regulation in LV grids by coordinated var-vol control strategies’, *J. Mod. Power Syst. Clean Energy*, 2014, **2**, pp. 419–328

[5] Alatrash, H., Amarin, R.A., Lam, C.: ‘Enabling large-scale PV integration into the grid’. Proc. IEEE Green Technologies Conf., Tulsa, OK, USA, April 2012

[6] Fuchs, A., Demiray, T.: ‘Large-scale PV integration strategies in distribution grids’. Proc. IEEE PowerTech, Eindhoven, Netherlands, June 2015

[7] Bouzguenda, M., Gastli, A., Al Badi, A.H., *et al.*: ‘Solar photovoltaic inverter requirements for smart grid applications’. Proc. IEEE Power and Energy Society Conf. Innovative Smart Grid Technologies – Middle East, Jeddah, Saudi Arabia, December 2011

[8] Katiraei, F., Aguero, J.R.: ‘Solar PV integration challenges’, *IEEE Power Energy Mag.*, 2011, **9**, pp. 62–71

[9] Vargas, J.P., Goss, B., Gottschalg, R.: ‘Large scale PV systems under non-uniform and fault conditions’, *Sol. Energy*, 2015, **116**, pp. 303–313

[10] Botelho de Almeida, J.O.M., Tôrres, A.G., Cupertino, A.F., *et al.*: ‘Three-phase photovoltaic inverters during unbalanced voltage sags: comparison of control strategies and thermal stress analysis’. Proc. IEEE Int. Conf. Industry Applications, Curitiba, Brazil, November 2016

[11] Energinet: ‘Technical regulation 3.2.1 for power plants up to and including 11 kW’, Doc. no. 15/01353-94, 2016